Dependence of the covalency of the $(MnF_6)^{4-}$ complex ion upon the Mn^{2+}-F^- distance

M. T. Barriuso
Departamento de Física Teórica, Facultad de Ciencias, Universidad de Cantabria, 39005 Santander, Spain

J. A. Aramburu and M. Moreno
Departamento de Optica y Estructura de la Materia, Facultad de Ciencias, Universidad de Cantabria, 39005 Santander, Spain

M. Flórez, G. Fernández Rodrigo, and L. Pueyo
Departamento de Química Física y Analítica, Facultad de Química, Universidad de Oviedo, 33007 Oviedo, Spain
(Received 10 September 1987)

The covalency of the $(MnF_6)^{4-}$ cluster has been examined by means of cluster-*in-vacuo* and cluster-in-the-lattice Hartree-Fock-Roothaan (HFR) calculations. The lattice potentials of $RbMnF_3$ and $KMgF_3$ have been considered. We have found that the covalency parameters f_s and $f_p = f_\sigma - f_\pi$ change as the Mn^{2+}-F^- distance R changes from 1.90 to 2.32 Å, as $R^{-8.2}$ and $R^{-3.2}$, respectively. This result might be helpful in future determinations of these parameters under high pressure. Several contributions to the covalency of the Mn^{2+}—F^- bond, including the $3d$-orbital deformation, the action of the empty $4s$ and $4p$ metallic orbitals, and the effects of the crystal lattice, have been analyzed from the HFR wave function. Calculations show that, these three contributions being small, the $(MnF_6)^{4-}$ complex is highly ionic and its A_s and A_p superhyperfine constants behave as local observables, i.e., changes in their observed values from crystal to crystal are mainly determined by changes in the Mn^{2+}-F^- distance. The traditional analysis of the superhyperfine tensor directed to obtain empirical covalency parameters has also been reexamined. Quantitative evaluation of the often-neglected metal-ligand terms and fluoride relaxation accompanying impurity substitution has shown that these two factors play a key role in determining the anisotropic covalency parameters from magnetic-resonance data. From electron-nuclear double-resonance measurements in cubic fluoroperovskites doped with Mn^{2+}, we have found $f_p = 0.60 \pm 0.20\,\%$. The new empirical values of f_p derived in this work for Mn^{2+}:$KZnF_3$, Mn^{2+}:$RbCdF_3$, and Mn^{2+}:$CsCaF_3$ do not show a definite trend when R changes. More experimental work is needed to determine the nature of this variation.

I. INTRODUCTION

The magnetic and optical properties of transition-metal compounds depend, at a microscopic level, upon the electron delocalization or covalency of the metal-ligand bond. In order to understand the variations produced in these properties by changes in the crystalline environment or by external perturbations like hydrostatic pressure or temperature, one must know how the covalency changes with the metal-ligand distance R.

The traditional theory of the metal-ligand covalency[1] was developed under the molecular-orbital linear-combination-of-atomic-orbitals (MO LCAO) approximation. In this approach, the covalency of a one-electron MO wave function ψ is given by covalency parameters which measure the degree of mixing between metal and ligand atomic orbitals (AO's) in ψ. For instance, in octahedral complexes[1] the metallic $3d$ AO's split into $3dt_{2g}$ and $3de_g$ orbitals and mix with symmetry-adapted ligand functions of $t_{2g}(\chi_\pi)$ and $e_g(\chi_s,\chi_\sigma)$ symmetry, respectively. The covalency parameters λ_s, λ_σ, and λ_π measure the $3de_g$-χ_s, $3de_g$-χ_σ, and $3dt_{2g}$-χ_π mixing, respectively. The unpaired-spin density at the ligand sites, as transferred from the metallic orbitals, is usually given by the spin-density (or, in a broad sense, covalency) parameters $f_s = (N_e\lambda_s)^2/3$, $f_\sigma = (N_e\lambda_\sigma)^2/3$, and $f_\pi = (N_t\lambda_\pi)^2/4$. In these expressions N_e and N_t are the normalization constants of the open-shell e_g and t_{2g} MO's, respectively.[1]

These parameters can be determined from magnetic-resonance spectroscopy, neutron diffraction, or nonempirical calculation. Electron-nuclear double-resonance (ENDOR) spectroscopy is the more suitable technique due to its high accuracy in the measurement of the superhyperfine (shf) tensor, the quantity giving the most direct information on the metal-to-ligand spin transfer.

The covalency of the $(MnF_6)^{4-}$ system has been investigated many times recently. Experimentally, a large number of fluoroperovskites containing Mn^{2+} has been explored by nuclear magnetic resonance (NMR) or electron paramagnetic resonance (EPR),[2-11] and some of them by ENDOR.[12-15] Most theoretical calculations[16-28] have been performed at a single value of R. Calculations at different distances[18,22,26,28] suggest that the isotropic parameter f_s decreases when R increases more steeply than the anisotropic quantity $f_p = f_\sigma - f_\pi$ does.

By contrast with what is known about f_s, the available experimental information on f_p is rather confusing for this system. In particular, its R dependence is not clear

at all. As an example, f_p increases by a factor larger than 3 from Mn^{2+}:$KZnF_3$ to Mn^{2+}:$CsCaF_3$, according to the recent results reported by Aoki *et al.*[13] Large variations from crystal to crystal can also be seen in the work by Emery *et al.*[27] on fluorperovskites containing Mn^{2+}. These sharp variations contrast with experimental and theoretical results for other compounds. Available theoretical calculations give also large variations for f_p, in contrast with what is found for f_s. Theoretical values of f_p from 0.40% (Ref. 28) to 2.42% (Ref. 19) have been reported.

In view of this contradictory situation we have reexamined the covalency of the Mn^{2+}—F^- bond, with particular attention to the question of the R dependence of f_s and f_p. We have performed near-*ab-initio* Hartree-Fock-Roothaan (HFR) calculations on the $(MnF_6)^{4-}$ cluster at several values of R by means of an improved version of the open-shell self-consistent field (SCF) MO methodology developed by Richardson *et al.*[29] Using the HFR wave function, we have analyzed the effects on the R dependence of these parameters of important mechanisms of electron delocalization such as the $3d$-orbital deformation, the presence of the $4s$ and $4p$ metallic AO's in the SCF space, and the cluster-lattice interaction.

The result of this calculation is that f_s and f_p decrease uniformly when R increases, f_s as $R^{-8.2}$ and f_p as $R^{-3.2}$. Both predictions, deduced from cluster-*in-vacuo* calculations, are practically unchanged when an accurate representation of the point-charge lattice potential of $RbMnF_3$ and $KMgF_3$ is included in the cluster Hamiltonian. This suggests that f_s and f_p, and their related shf constants A_s and A_p, are local observables, their values being mainly determined by intracluster interactions. This result also justifies the idea of determining equilibrium Mn^{2+}-F^- distances from the observed values of A_s,[30] and suggests that the cluster-*in-vacuo* predictions discussed here might apply to analogous manganese fluorides as well. The presence of the $4s$ and $4p$ AO's in the SCF space has also minor effects on the R dependence of the covalency parameters. Furthermore, the predicted variation of f_s with R and the numerical value of this parameter at the equilibrium metal-ligand distance are in very good agreement with the experimental information and with previous calculations.

On the other hand, we find that whereas the $f_p(R)$ function deduced from the HFR calculations is smooth, the ENDOR values of f_p for fluoroperovskites[12–14] show an erratic variation with R. This noticeable difference between f_s and f_p directed us to reexamine the method of obtaining the covalency parameters from nuclear-magnetic-resonance data. We have found that two contributions usually neglected in previous analyses, namely, the ligand relaxation induced upon impurity substitution, and the metal-ligand terms of the shf Hamiltonian, play a very important role in the final value of the covalency parameters.

Given the importance of these contributions, we present here the details of the accurate analysis of the magnetic-resonance data. In order to determine the ligand relaxation, we have taken the true metal-ligand distance in the doped crystals from extended x-ray-absorption spectroscopy (EXAFS) measurements[31] when available. Otherwise, we have calculated this distance from the observed isotropic shf constant[30] and crystal-field spectrum.[32,33] Furthermore, we have calculated the two-center terms accurately by numerical quadratures.

In this way, the ENDOR data for Mn^{2+}:$KZnF_3$ ($R_e=2.07\pm0.01$ Å), Mn^{2+}:$RbCdF_3$ ($R_e=2.12\pm0.01$ Å), and Mn^{2+}:$CsCdF_3$ ($R_e=2.16\pm0.01$ Å) give $f_p=0.56\pm0.20\%$, $0.49\pm0.21\%$, and $0.73\pm0.21\%$, respectively, i.e., $f_p=0.60\pm0.20\%$ in the range $2.07\leq R\leq 2.16$ Å. The contribution of the ligand relaxation to these values of f_p is quite large and clearly determines the R dependence of the parameter. The metal-ligand terms are also important in determining the final value of f_p but have a smaller effect in its R dependence.

The new empirical values of f_p presented here are fairly consistent with the valence-bond calculation by Shrivastava,[26] and the approximate HFR calculations by Emery and Fayet.[28] Our HFR prediction turns out to be rather high, probably due to an underestimation of f_π assignable to limitations of our theoretical scheme. The small size of our basis set may be one of the more important among such limitations.

In the next section we make a brief summary of previous calculations of the covalency of the $(MnF_6)^{4-}$ ion. Our SCF calculations and results have been collected in Sec. III. In the last section we present the MO LCAO analysis of the shf tensor and show the significant effects of ligand relaxation and two-center terms on the empirical covalency parameters.

II. PREVIOUS THEORETICAL CALCULATIONS OF THE COVALENCY OF $(MnF_6)^{4-}$

Since we will concentrate on the variation of the covalency parameters with the metal-ligand distance, we collect in Table I numerical values reported in previous calculations performed at more than one distance. Some other important theoretical works containing calculations at a single value of R are also commented below.

Brown and Burton[18] reported the first calculation of the spin density of the $(MnF_6)^{4-}$ cluster at several values of R. They performed approximate unrestricted Hartree-Fock calculations on several transition-metal clusters, both *in vacuo* and inside the electrostatic potential of "isolated-cluster" lattices, such as K_2NaCrF_6, and "shared-cluster" lattices, such as the perovskites $KMnF_3$ and $RbMnF_3$. In general, they found uniformly small effects of the electrostatic lattice potentials on the computed spin densities of the cluster. They argued that for increasing values of R one would expect the π covalency to decrease more rapidly than the σ covalency, and so expect f_p to increase with R. Their results show, however (see Table I), that f_p is rather sensitive to changes in R, decreasing when R increases. They found f_σ to be about 7 times larger than f_π.

Larsson[22] reported multiple-scattering $X\alpha$ calculations on $(MnF_6)^{4-}$ at 2.09 and 2.67 Å. We collect his results

for the antibonding e_g MO. The e_g density decreases slightly when R increases. According to his spin-polarized results, the occupied a_{1g} MO's do contribute to the transferred spin density. The spin-up a_{1g} MO shows a larger 4s-ligand mixture than the spin-down MO, removing spin-up density from the $2p_\sigma$-ligand orbitals and decreasing f_σ. This mechanism is of little significance at the usual equilibrium value of $R(Mn^{2+}\text{-}F^-)$ in cubic fluoroperovskites but it becomes very important at $R=2.67$ Å, the equilibrium distance of the pure KF host lattice. At such a value of R the negative a_{1g} contribution and the positive e_g value are very similar, producing a total f_σ close to zero.

Shrivastava[26] computed the covalency for the Mn^{2+}-F^- dimer and the Mn^{2+}-F^--Mn^{2+} trimer at various metal-fluoride distances by means of a valence-bond scheme. This author finds, for the dimer, an increasing f_p from 1.90 to 2.0 Å and then a stabilization around $f_p=0.46\%$ from 2.0 to 2.2 Å. These results follow the idea of Brown and Burton of a π covalency decreasing faster than the σ covalency.

In Table I we include the approximate HFR results of Emery and Fayet[28] that predict a very slight dependence of f_p with R. As we can see in the table, the numerical values of f_p given by these authors are in very good agreement with those reported by Shrivastava for the Mn^{2+}-F^- dimer[26] but they are about 4 times smaller than those found by Brown and Burton[18] and by Larsson.[22]

Some other theoretical results obtained at $R=2.12$ Å deserve comment. Soules and Richardson[19] find $f_\sigma=2.90\%$ and $f_\pi=0.48\%$ in the restricted HFR description. They report that spin polarization reduces the value of f_σ to 1.96% and increases f_π to 0.74%, reducing f_p from 2.42 to 1.22%. The two-center or overlap effects reduce f_σ further to 1.49%, giving $f_p=0.75\%$ as the best prediction. Frozen-core, restricted HFR calculations on the $(MnF_6)^{4-}$ cluster *in vacuo* were reported by Matsuoka.[20,21] In these calculations, f_s can change from 0.58% to 0.48%, f_σ from 1.32% to 1.64%, and f_π from 0.25% to 0.36%, depending upon the degree of refinement, but the value of $f_\sigma-f_\pi$ remains relatively stable around 1.20%. Substituting of all core electrons by point charges reduces f_σ to 0.79% and f_π to 0.20%, and consideration of the 4s metallic AO's produces only slight effects on the covalency parameters. f_s remains in-

TABLE I. Different theoretical calculations, in percent of f_s (first row), f_σ (second row), f_π (third row), and $f_p=f_\sigma-f_\pi$ (fourth row) at several distances. Results by Larsson and Brown and Burton do not include f_s. (a) Mn^{2+}-F^- dimer. (b) Mn^{2+}-F^--Mn^{2+} trimer system. (c) Contribution from the e_g MO. (d) Cluster-*in-vacuo*, SPDDSP calculation.

Author	Ref.			R (Å)		
Shrivastava	26	1.90	2.00	2.10	2.20	
	(a)	1.1423	0.8648	0.6421	0.4532	
		0.9130	0.8518	0.7642	0.6652	
		0.6368	0.4380	0.2973	0.2017	
		0.2762	0.4138	0.4669	0.4635	
	(b)	1.0308	0.7417	0.5122	0.3382	
		0.7583	0.6639	0.5562	0.4632	
		0.7566	0.5383	0.3842	0.2724	
		0.0017	0.1256	0.1720	0.1908	
Emery and Fayet	28		1.1	0.78	0.51	
			3.45	2.80	2.27	
			3.10	2.40	1.90	
			0.35	0.40	0.37	
Larsson	22			2.093		2.673
	(c)			2.40		1.50
				0.70		0.30
				1.70		1.20
Brown and Burton	18			2.093	2.121	
				2.183	1.882	
				0.294	0.246	
				1.889	1.636	
This work		1.905	2.011	2.117	2.223	2.328
	(d)	1.442	0.956	0.635	0.420	0.277
		4.619	3.816	3.149	2.584	2.100
		1.018	0.705	0.478	0.319	0.211
		3.601	3.111	2.671	2.265	1.889

sensible to all these changes. Adachi *et al.*[25] obtained $f_s=0.22\%$, $f_\sigma=1.4\%$, and $f_\pi=0.6\%$ from a discrete variational $X\alpha$ calculation on $KMnF_3$. Clack and Monshi[24] reported complete-neglect-of-differential-overlap (CNDO) and intermediate-neglect-of-differential-overlap (INDO) calculations for $(MnF_6)^{4-}$ at the observed geometry. Their CNDO results are $f_s=0.34\%$, $f_\sigma=2.45\%$, and $f_\pi=0.20\%$, and their INDO values are $f_s=0.10\%$, $f_\sigma=1.63\%$, and $f_\pi=0.10\%$.

These results reveal a different sensitivity of the theoretical f_s and f_p against methodological refinements. For instance, the HFR calculations give $f_s=0.5\pm0.1\%$ whereas f_p shows variations from 0.4% to 2.4%. It is interesting to recall that the experimental values of f_s cluster around 0.5% whereas those of f_p scatter from 0.12% to 0.98%.[13] It appears then that the observed value of f_s is stable and that HFR theory is able to reproduce it. By contrast, f_p seems to be difficult to determine either from theory or experiment. Thus, further study of f_p is necessary.

III. NEW HARTREE-FOCK-ROOTHAAN RESULTS

Let us now examine our HFR calculations. A short preliminary report has been presented elsewhere.[34] These calculations have been performed by means of an improved version of the open-shell HFR methodology of Richardson *et al.*[29] The Slater-type orbital (STO) basis sets of Refs. 35 and 36 have been used for describing the metallic AO's. The fluoride basis set is that used in the recent calculation of the optical spectrum of the $(MnF_6)^{4-}$ ion by Flórez *et al.*[37] Some important modifications incorporated in the version used here permit the study of the theoretical mechanisms described in the Introduction. Briefly, these changes are as follows.

(a) The valence shell can now simultaneously contain the 3*s*, 3*p*, 3*d*, 3*d'*, 4*s*, and 4*p* metallic AO's, as described in Refs. 37 and 38. The function called 3*d'* is the inner STO of the 2ζ regular 3*d* AO of Ref. 35. It gives rise to slightly enlarged t_{2g} and e_g MO's, as commented above, giving flexibility to the basis set and allowing for the study of the 3*d*-orbital deformation associated with the metal-ligand bonding. This enlarged valence shell will be called SPDDSP.

(b) Ligand-ligand interactions are accurately computed by means of a procedure called renormalization and described by Kalman and Richardson.[39] This refinement becomes particularly relevant for voluminous ligands but it is also necessary for compact ligands like the fluoride ions at very short metal-ligand distances.

(c) The core projection introduced by Huzinaga and collaborators[40] has been included. This operation enforces the necessary core-valence orthogonality in frozen-core calculations and, as discussed in Refs. 41 and 42, it plays a key role in the accurate prediction of the equilibrium geometry of the cluster.

(d) The cluster-lattice interaction has been simulated in terms of the point-charge approximation. The point-charge lattice potential, calculated by the Ewald method at many points of the cluster volume, has been represented by an accurate one-electron operator and introduced in the Fock equations before self-consistency. Details on this treatment of the cluster-lattice interaction have been given in Refs. 43 and 44.

Core-projected, renormalization calculations have been performed for the ${}^6A_{1g}$ electronic ground state of the $(MnF_6)^{4-}$ unit at several values of the metal-ligand separation. Cluster-*in-vacuo* results have been complemented with various cluster-in-the-lattice calculations corresponding to the $RbMnF_3$ and $KMgF_3$ perovskites. The results of our calculations involving two 3*d* functions have been transformed into the traditional MO LCAO formalism in order to make the comparison with the empirical covalency parameters meaningful.

Before passing to discuss the results we would like to recall that this restricted HFR methodology is of an approximate nature. Its main limitations can be related to the reduced basis set, lack of electron correlation, and the electrostatic representation of the lattice ions.

In defense of these criticisms we can argue, first, that the metallic basis set is a faithful simulation of a high-quality basis.[35,36] The ligand basis may be too compact around the ligand nucleus but it gives a reasonable representation of the fluoride electron density in the lattice.[45] Electron correlation effects may be important in determining the ground-state energy. However, our calculated ground-state nuclear potential gives an equilibrium Mn^{2+}-F^- distance in very good agreement with the observed data.[46] On the other hand, the observed *g* values for Mn^{2+}-doped fluoroperovskites[2] are practically equal to g_0, $|g-g_0|$ being less than 2.0×10^{-3}. This suggests that the mixture of the ${}^6A_{1g}$ ground state with excited electronic states is negligible for this d^5 ion and that the diagonal HFR description of this work is reasonable. Finally, a rigorous quantum treatment of the cluster-lattice interaction is very expensive.[43] Preliminary calculations with sophisticated lattice models which include Coulomb, nonlocal exchange, and lattice projection operators, indicate[47] that the lattice effects on the cluster electron density may be moderate in Mn^{2+}-containing cubic fluoroperovskites. Clearly, further lattice effects could appear in cluster calculations with lattice models containing electronic and geometrical relaxations of the lattice ions (lattice polarization) due to impurity substitution.

Thus, the present methodology represents a compromise between high quality and economy that gives rather accurate results for many observable properties. In principle, it appears as an appropriate tool for the study of the important covalency-related questions advanced in the Introduction. It is necessary to recall, however, that the calculation of the covalency parameters involves the determination of rather small quantities from the internal structure of the cluster-variational wave function. Since the variational method ensures a total electronic energy stable against small variations of the wave function, we can think of two slightly different wave functions giving essentially the same electronic energy and still predicting noticeably different covalency parameters. From the variational viewpoint, these two functions would be equally acceptable. This reminds us that the accurate calculation of covalency parameters by means of

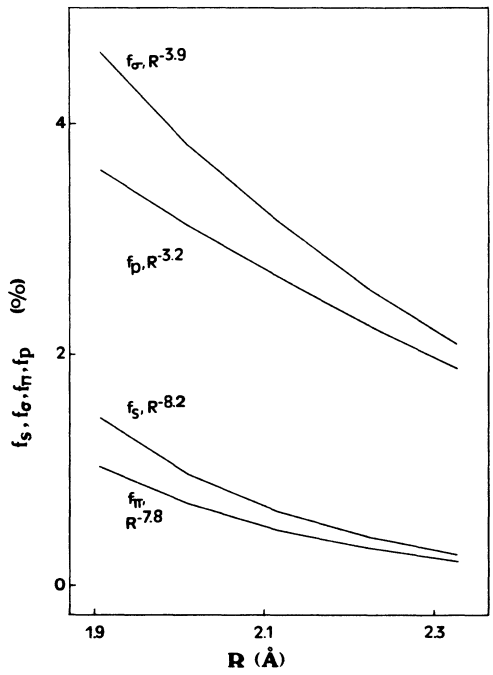

FIG. 1. SPDDSP cluster-*in-vacuo* calculation of the f_s, f_σ, f_π, and f_p covalency parameters at several metal-fluoride distances.

nonempirical variational procedures is a difficult task.

Let us see now the results of our study.

A. The R dependence of the covalency parameters

In Fig. 1 we present the R dependence of the f_s, f_σ, f_π, and f_p parameters for the $(MnF_6)^{4-}$ cluster, as obtained from the SPDDSP cluster-*in-vacuo* calculations. Notice that the range of R in this figure is much larger than that observed experimentally. These variations can be well approximated by the inverse-power functions $f_i = AR^{-n}$ $(i = s,\sigma,\pi,p)$. In Fig. 1 we show the best values for the exponent n in each case.

We can see the sharp variation of f_s with R, in remarkable agreement with the results of Shrivastava (R^{-7}) (Ref. 26) and Emery, Leblé, and Fayet ($R^{-9.5}$) (Ref. 27). Furthermore, f_p changes with R much more slowly than f_s does. As commented below, this difference in the R dependence of f_s and f_p is essentially insensitive to the action of the cluster-lattice interaction. For that reason the $f_s(R)$ and $f_p(R)$ theoretical curves in Fig. 1 might be useful in future determinations of covalency parameters under high pressure.

B. The local character of f_s and f_p

In Table II we see that both f_s and f_p computed for Mn^{2+}:$KMgF_3$ and Mn^{2+}:$RbMnF_3$ differ from the cluster-*in-vacuo* values by less than 15% in the worst case ($R = 2.328$ Å). These differences are less than about 6% near the usual equilibrium value of R (2.117 Å). Such modest lattice effects are comparable in magnitude to those obtained by Brown and Burton,[18] although the cluster-lattice interaction reduces the value of f_p in our calculation and increases it in that of Brown and Burton. We can conclude that the lattice potential of the cubic fluoroperovskites simulated by means of the point-charge approximation and the Ewald method modifies very slightly the cluster electron density. This result indicates that both f_s and f_p may be considered as local observables whose values should be determined by the intracluster interactions. Thus, the related quantities A_s and A_p would also be local, i.e., changes detected in A_s and A_p from crystal to crystal might more be attributed to changes in the cluster size than to specific effects of the crystal lattice. Following this idea, we have undertaken the analysis of the next section where we will understand the changes observed in A_p as produced by different true metal-fluoride distances in the cluster.

C. The proportionality between λ_s and the $\langle 3de_g \mid 2s_F \rangle$ overlap

Our results show that in $(MnF_6)^{4-}$ the $3de_g$-$2s_F$ interaction is essentially an overlap interaction with very small covalency contributions.[34] This leads to a proportionality between the covalency parameter λ_s and the

TABLE II. Covalency parameter f_s (first row) and $f_p = f_\sigma - f_\pi$ (second row) computed with different degrees of refinement. See text for definition of the valence shells SPD, SPDD, and SPDDSP.

			R (Å)		
Calculation	1.905	2.011	2.117	2.223	2.328
SPDDSP, *vacuo*	1.442	0.956	0.635	0.420	0.277
	3.601	3.111	2.671	2.265	1.889
SPDD, *vacuo*	1.434	0.947	0.627	0.416	0.274
	3.975	3.513	3.137	2.820	2.543
SPD, *vacuo*	1.455	0.952	0.624	0.408	0.264
	3.749	3.179	2.706	2.299	1.945
SPDDSP, $RbMnF_3$	1.456	0.971	0.651	0.437	0.293
	3.550	3.038	2.572	2.139	1.738
SPDDSP, $KMgF_3$	1.464	0.980	0.660	0.447	0.303
	3.516	2.990	2.508	2.062	1.647

$S_s = \langle 3de_g \mid 2s_F \rangle$ overlap integral, i.e., $\lambda_s = c_s S_s$. According to our results, the proportionality constant $c_s = 1.21 \pm 0.02$ for $2.07 \leq R \leq 2.16$ Å.[34] These results agree with those by Emery, Leblé, and Fayet,[27] and theoretically justify the use of the A_s method[30] for determining the true metal-ligand distances in Mn^{2+}-doped fluoroperovskites. Knowledge of this distance permits the incorporation of the fluoride relaxation in the calculation of the empirical f_p parameters, a very important part of the analysis presented in the next section.

D. The small 3*d*-orbital deformation in $(MnF_6)^{4-}$

This deformation can be estimated by comparing the SPDD and SPD results of Table II. The former differ from the SPDDSP ones in that the 4*s* and 4*p* AO's have been removed from the calculation. SPD basis is the SPDD one with the 3*d'* AO removed. This comparison reveals that the 2*p*-3*d* covalency is larger in the SPDD basis and that the effect increases with R. Near the equilibrium region ($R = 2.117$ Å) the second 3*d* AO increases f_p by about 16%. The effects of 3*d'* on f_s are much smaller, as shown in Table II.

This 3*d*-orbital deformation can also be appreciated by means of the transformation of the DD MO's into the traditional form.[1] Such transformation means a reduction from two 3*d* AO's to a single 3*d* function, called here $3d^{MO}$ to remember its origin. This $3d^{MO}$ function is *not* the free-ion AO but can be deduced from it by radial scaling.[37] In this way, we find a theoretical scaling or nephelauxetic[48] parameter *per* open-shell MO and metal-ligand distance. Briefly, the free-ion $3d_M(r)$ AO can be scaled into the $3d_M(\omega r)$ form which must resemble as closely as possible the $3d^{MO}$. This scaling parameter can thus be estimated by maximizing the $\langle 3d_M(\omega r) \mid 3d^{MO} \rangle$ overlap integral. In this way we obtain $\omega(e_g)$ and $\omega(t_{2g})$ for the open-shell e_g and t_{2g} MO's, respectively. Values of these scaling parameters are collected in Table III from 1.905 to 2.328 Å. We observe that the t_{2g} orbital expands and the e_g one contracts. The deformation is in any case very small.

This information is relevant in analyses of the magnetic-resonance data, such as those presented in the next section, where metallic wave functions are required. According to the present calculation, the use of free-ion orbitals for the Mn^{2+} ion in these analyses would be a reasonable choice.

E. The high ionicity of the $(MnF_6)^{4-}$ ion

The small 3*d*-orbital deformation just discussed also suggests that the normalization constants of the traditional MO's,[1] see Eqs. (2) and (3), are very close to unity. These constants have also been collected in Table III. This numerical result supports the use of $N_t = N_e = 1$ in the next section.

The small 3*d*-orbital deformation can also be seen as an indication of the highly ionic character of this complex. It is clear that the larger the covalency parameters the greater the separation of the normalization constants from unity. Thus, expression of our results in the form of Eqs. (2) and (3) confirms that $(MnF_6)^{4-}$ is highly ionic. Analogous results are deduced from the nonempirical calculation of different covalency-related properties, such as the orbital-angular-momentum reduction factors and g factors. These calculations indicate that the isoelectronic $(MnF_6)^{4-}$ and $(CrF_6)^{5-}$ systems are highly ionic, more than the $(CrF_6)^{4-}$, $(CrF_6)^{3-}$, and $(VF_6)^{4-}$ ions.[34,49]

F. The effects of the 4*s* and 4*p* empty AO's

These effects can be deduced by comparing the SPDDSP and the SPDD calculations. f_s is practically insensitive to the presence of these AO's. The differences in f_p are not great, although they are larger than those due to the lattice potential, particularly at larger distances. Still smaller effects of the 4*s* AO on f_s and f_p were found by Matsuoka.[20] Inclusion of 4*s* and 4*p* AO's in the calculation may decrease the 3*d*-ligand covalency as a consequence of the competition in the ligand-to-metal charge transfer between the traditionally considered e_g and t_{2g} channels, on the one hand, and the new channels open in the $a_{1g}(4s)$ and the $t_{1u}(4p)$ blocks by these virtual AO's, on the other. This slight reduction of the 3*d* covalency parameters may well cancel out the small increase due to the 3*d* deformation.

In summary, the present calculation gives a value for f_s (0.635% at 2.117 Å) in good agreement with the experiment. We find that this parameter varies with R as $R^{-8.2}$, in reasonable agreement with earlier theoretical results by Shrivastava (R^{-7}) (Ref. 26) and Emery *et al.* ($R^{-9.5}$) (Ref. 27). The prediction value for f_p near R_e is somewhat high (2.671% at 2.117 Å), possibly due to an underestimation of f_π related to the small size of our basis. We have also studied several interesting phenome-

TABLE III. Normalization constants and scaling factors computed at several metal-fluoride distances. SPDDSP cluster-*in-vacuo* calculations.

	R (Å)				
	1.905	2.011	2.117	2.223	2.328
N_e	1.0102	1.0018	0.9961	0.9928	0.9911
$\omega(e_g)$	1.011	1.009	1.006	1.004	1.001
N_t	0.9989	0.9981	0.9980	0.9983	0.9986
$\omega(t_{2g})$	0.971	0.976	0.979	0.982	0.984

na related to the covalency of the Mn^{2+}—F^- bond. Our HFR predictions on 3*d*-orbital deformation, the role of 4*s* and 4*p* AO's, normalization constants of the MO's, and lattice effects, serve as a guide for improving the current theoretical analysis of the magnetic-resonance data. We proceed to this analysis in the next section.

IV. COVALENCY PARAMETERS FROM MAGNETIC-RESONANCE SPECTROSCOPY

In the restricted HFR formalism, the open-shell part of the $t_{2g}(3)e_g(2)\,^6A_{1g}$ ground state of the $(MnF_6)^{4-}$ unit can be written as a single-determinant wave function:[50]

$$|\,^6A_{1g}, M_S=\tfrac{5}{2}\rangle = |\,\xi^+\eta^+\zeta^+\theta^+\epsilon^+\rangle = |\,\xi\eta\zeta\theta\epsilon\rangle\,|\,S=\tfrac{5}{2}, M_S=\tfrac{5}{2}\rangle\ , \quad (1)$$

ξ, η, and ζ being the three t_{2g} MO's, and θ and ϵ the two e_g MO's.

These MO's can be written in the form[1]

$$|\,e_g\gamma\rangle = N_e\{\,|\,3d\gamma\rangle - \lambda_\varsigma\,|\,\chi_\varsigma\rangle - \lambda_\sigma\,|\,\chi_\sigma\rangle\}\ , \quad (2)$$

$$|\,t_{2g}\gamma\rangle = N_t\{\,|\,3d\gamma\rangle - \lambda_\pi\,|\,\chi_\pi\rangle\}\ , \quad (3)$$

where γ is the symmetry subspecies and χ_ς, χ_σ, and χ_π symmetry-adapted ligand functions.

The spin-orbit coupling can mix this sextet with excited electronic states. This mixing is responsible for the observed *g* shifts and, in principle, it cannot be neglected in the analysis of the shf tensor. In Cu^{2+}:$CdCl_2$, for instance, $g_\parallel = 2.33$ and the spin-orbit mixing of the ground state contributes about 25% to the experimental A_p (Ref. 51). However, for the $(MnF_6)^{4-}$ ion this modification of the ground state is very small. The mixing with the $^4T_{1g}$ states from the d^5 configuration is small due to the large difference between the spin-orbit constant and the corresponding electronic energy separation. The mixing with charge-transfer states would still be less important since these states lie several eV above the ground state.[52,53] As commented above, the observed *g* values[2] for Mn^{2+}-doped fluorperovskites are practically equal to g_0. In view of this, we will accept as good the diagonal representation of the electronic ground state given by Eq. (1).

The spin Hamiltonian appropriate to describe the ground state of a complex ion like $(MnF_6)^{4-}$ contains the shf term

$$H_{\rm shf} = \sum_{k=1}^{6} \vec{S}\cdot\vec{\vec{T}}^{\,k}\cdot\vec{I}_k\ , \quad (4)$$

reflecting the effective coupling between the electron spin $\vec{S}$ and the spin $\vec{I}_k$ of the ligand nucleus placed at $\mathbf{R}_k$. For the present case, the shf tensor $\vec{\vec{T}}^{\,k}$ is diagonal in its local reference frame (x',y',z'), see Fig. 2. Then $T_{x'x'} = T_{y'y'} = A_\perp$ and $T_{z'z'} = A_\parallel$.

The anisotropic part of the shf tensor, $A_p = (A_\parallel - A_\perp)/3$, comes from the magnetic dipolar coupling term, H_D^k, between the unpaired electron spin and the nuclear spin of the *k*th ligand ion:

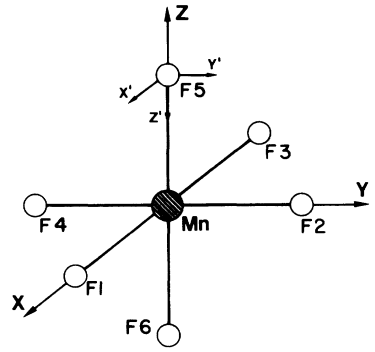

FIG. 2. Definition of coordinate system.

$$H_D^k = 2g_L\beta\beta_N\sum_i[3(\mathbf{r}_i'\cdot\vec{\mathbf{s}}_i)(\mathbf{r}_i'\cdot\vec{\vec{\mathbf{I}}}_k)(\mathbf{r}_i')^{-5} - \vec{\vec{\mathbf{I}}}_k\cdot\vec{\mathbf{s}}_i(\mathbf{r}_i')^{-3}]\ , \quad (5)$$

where g_L corresponds to the ligand nucleus, the sum involves all the unpaired electrons of the complex, and $\mathbf{r}_i' = \mathbf{r}_i - \mathbf{R}_k$. In this work we shall refer the shf interaction to the ligand F5, as depicted in Fig. 2.

The quantities $A_\parallel$ and $A_\perp$ appearing in the spin Hamiltonian are related to the expectation value of H_D^k in the electronic ground state. In particular, A_p is given by

$$2A_p = 2g_L\beta\beta_N(1/2S)\left\langle {}^6A_{1g}\left|\sum_i[3(z_i')^2-(r_i')^2]\times(r_i')^{-5}\right|{}^6A_{1g}\right\rangle\ , \quad (6)$$

where the sum runs over the five unpaired electrons.

Equation (6) gives rise to a sum over the five MO's appearing in Eq. (1). In our calculation we have neglected the ligand-ligand integrals given the inner character of the operator H_D^k. On the other hand, the metal-ligand and metal-metal interactions have been computed accurately.

The final form of A_p becomes

$$A_p = A_d - A_{\rm ML} + A_\sigma - A_\pi\ . \quad (7)$$

Here

$$A_\sigma - A_\pi = (f_\sigma - f_\pi)A_p^0/5 \quad (8)$$

is the covalent contribution coming from the unpaired spin density transferred into ligand F5. $A_p^0 = 428.6\times10^{-4}\ \mathrm{cm}^{-1}$ corresponds to the free fluoride ion, as obtained with a Clementi and Roetti basis set.[54]

The metal-ligand, two-center, or overlap contribution term $A_{\rm ML}$ has usually been neglected in previous analysis. Its expression is

$$A_{\rm ML} = 2g_L\beta\beta_N\tfrac{1}{5}[N_e f_\sigma^{1/2}\langle 3d_{z^2}\,|\,D_{z'z'}\,|\,-2p_z(5)\rangle + 2N_t f_\pi^{1/2}\langle 3d_{yz}\,|\,D_{z'z'}\,|\,2p_y(5)\rangle + N_e f_s^{1/2}\langle 3d_{z^2}\,|\,D_{z'z'}\,|\,2s(5)\rangle]\ , \quad (9)$$

where $D_{z'z'}$ is the dipolar operator in Eq. (6). Analogous-

TABLE IV. Metal-ligand and metal-metal matrix elements of Eqs. (9) and (10), computed with the basis sets of Ref. 54.

R (a.u.)	$\langle 3d_{z^2} \mid D_{z'z'} \mid -2p_z(5)\rangle$	$\langle 3d_{z^2} \mid D_{z'z'} \mid 2s(5)\rangle$	$\langle 3d_{yz} \mid D_{z'z'} \mid -2p_y(5)\rangle$	$\langle 3d_{z^2} \mid D_{z'z'} \mid 3d_z^2\rangle$
3.00	0.137 910	0.043 740 5	0.010 566	0.104 579
3.20	0.106 065	0.033 778 0	0.007 128 14	0.083 639
3.40	0.081 361 7	0.025 930 9	0.004 824 13	0.067 734
3.60	0.062 307 2	0.019 811 2	0.003 277 94	0.055 521
3.80	0.047 675 5	0.015 078 4	0.002 237 09	0.046 033
4.00	0.036 478 3	0.011 443 8	0.001 533 90	0.038 577
4.20	0.027 931 0	0.008 668 66	0.001 056 61	0.032 649
4.40	0.021 418 0	0.006 576 90	0.000 731 37	0.027 925

ly, the dipolar or metal-metal term is given by

$$2A_d = 2g_L\beta\beta_N \tfrac{1}{5}\left[\sum_{\Gamma_\gamma=1}^{5} N_\Gamma^2 \langle 3d_{\Gamma_\gamma} \mid D_{z'z'} \mid 3d_{\Gamma_\gamma}\rangle\right], \quad (10)$$

and becomes

$$A_d^0 = (2g_L\beta\beta_N)/R^3, \quad (11)$$

if the $3d$ functions are approximated by δ functions and $N_e = N_t = 1$. In the range of distances considered in the present case the differences between A_d and A_d^0 are smaller than 2%. In the present analysis the dipolar term has always been computed by means of Eq. (10) with the normalization constants set to unity.

Based on the theoretical results noted in Sec. III D, all matrix elements in Eqs. (9) and (10) have been calculated numerically in polar and cylindrical coordinates centered at the nucleus F5 using *free-ion* AO's. Both the atomic basis sets[54] of Clementi and Roetti and the reduced bases used in previous section[35–37] have been considered. Differences between results from the two bases are always smaller than 20%. Some matrix elements computed with the high-quality bases[54] can be seen in Table IV. Final results given here for the f_p parameter will be those corresponding to the basis of Clementi and Roetti. We have checked our integration procedures by computing the matrix elements for the Al^{3+}-O^- system reported by Adrian *et al.*[55] Our results reproduce all figures in Ref. 55.

We can now analyze the influence of the dipolar and two-center contributions to the final value of f_p, for given values of A_p. In order to illustrate the separate actions of these terms we will present three levels of description.

(a) The dipolar term is computed by means of the approximate Eq. (11) using the metal-ligand distance of the host lattice. Furthermore, the two-center term is neglected. This scheme corresponds to the traditional analysis.[4]

(b) The ligand relaxation accompanying cationic substitution is included into the calculation of the dipolar term, whereas the two-center term is still neglected.

(c) Ligand relaxation and two-center contribution are accurately computed.

In this way, comparison of levels (a) and (b) will show the effects of ligand relaxation, and level (c) will reveal the contribution of an accurately computed overlap term.

As remarked above, we shall limit our analysis to the three Mn^{2+} fluoroperovskites for which ENDOR data are available. To execute level (b) we have taken the true metal-ligand distances from EXAFS data,[31] observed isotropic shf constants,[30] and crystal-field spectra.[32,33] The three methods lead to the same value of R within ± 0.01 Å.

Inclusion of level (c) from a pure empirical viewpoint presents a difficulty. As can be seen in Eq. (9), the two-center term depends upon f_s, f_σ, and f_π. Since f_s is immediately obtained from the observed A_s, Eq. (7) becomes, for an empirically known A_p, an equation with two unknowns: f_p and either f_σ or f_π. What is needed in this case is an estimation of the sensitivity of the two-center term to the variations of f_σ and f_π.

In order to examine this sensitivity, we can first express Eq. (7) as a function, for instance, of f_p and f_π, then assume a value for f_π, and finally solve the equation for f_p. This procedure gives us the variation of f_p with f_π as well as the variation of f_σ with f_π, for a given A_p. The results obtained for Mn^{2+}:$KZnF_3$, Mn^{2+}:$RbCdF_3$, and Mn^{2+}:$CsCaF_3$ are depicted in Fig. 3. We can observe

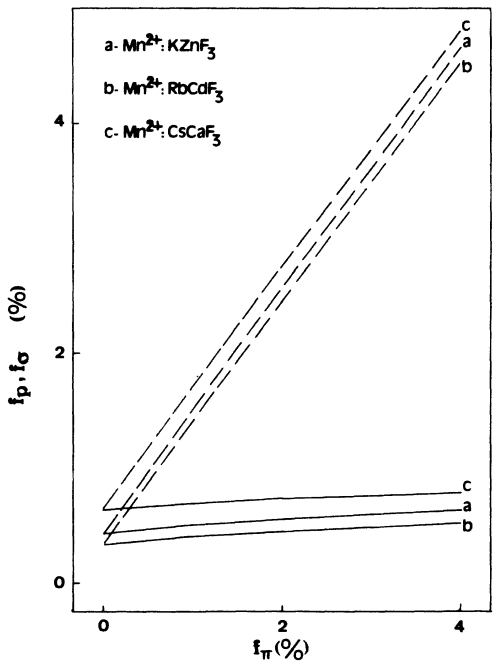

FIG. 3. Sensitivity of empirical f_p (solid lines) and f_σ (dashed lines) parameters to changes in f_π for three different systems, as predicted by Eq. (7).

that f_σ shows a steep dependence upon f_π but f_p is fairly insensitive to changes in f_π.

Furthermore, it is interesting to notice that whereas the uncertainty in A_{ML} introduces an uncertainty in the final value of f_p, the determination of the $f_p(R)$ function suffers much less from such uncertainty because the A_{ML} term is slightly dependent upon R. This circumstance makes the uncertainty in the A_{ML} to produce errors of about 0.05% in the final value of f_p.

Alternatively, this estimation of the precision achieved in f_p can be figured out from an analysis of Eq. (7) based on the assumption that f_σ lies between 1.0% and 3.3%. This range for f_σ can be justified in view of the following.

(a) Most theoretical calculations on $(MnF_6)^{4-}$ at the equilibrium geometry give f_σ values within this range, results by Shrivastava[26] and Emery *et al.*[27] being exceptions.

(b) Neutron-diffraction data for MnF_2 (Ref. 5) suggest that $f_\sigma < 3\%$ if $f_s \simeq 0.5\%$.

(c) The analysis of the spin Hamiltonian of K_2CuF_4 and $(NiF_6)^{4-}$ gives $f_\sigma = 4.2\%$ (Ref. 53) and 3.18,[4] respectively. As the optical electronegativities of Cu^{2+} ($\chi = 2.4$) and Ni^{2+} ($\chi = 2.1$) (Ref. 56) are higher than that determined for Mn^{2+} ($\chi = 1.4$),[53] we expect f_σ to be smaller for $(MnF_6)^{4-}$.

Let us see now the numerical results. The three levels of description referred to above have been summarized in Table V. In this table we collect, first, the values of A_p observed by ENDOR in three Mn^{2+}-containing fluoroperovskites. The metal-ligand distances in this Table are 0.01 Å smaller than those in Ref. 30 because the numbers in this reference were determined at room temperature and the ENDOR data in Table V have been obtained at low temperature. The next three columns correspond to the first approximation: $A_{ML} = 0$ and $R = R_0$, the distance of the host lattice. The resulting values of f_p show a great variation with R, from 0.12% at 2.026 Å to 0.92% at 2.262 Å. According to this level of description f_p increases abruptly with R.

The next three columns in Table V contain results of level (b): $A_{ML} = 0$ and ligand relaxation included. Since the lattice relaxation can be as large as 0.1 Å ($CsCaF_3$), the dipolar term A_d, varying as R^{-3}, can change from 2.12 to 2.45, in units of 10^{-4} cm^{-1}. This produces a very substantial change in f_p and more particularly in the $f_p(R)$ function. Now f_p decreases slightly from $KZnF_3$ (2.07 Å) to $RbCdF_3$ (2.12 Å) and shows a sharp turn in passing to $CsCaF_3$.

Finally, we find level (c) which includes the calculation of A_{ML}. In the table we can see that this overlap term is an order of magnitude smaller than A_p and A_d, but comparable with the difference $A_p - A_d$. This is the reason for the very large effects of this term in the final values of f_p. We notice that f_p still decreases from $KZnF_3$ to $RbCdF_3$ and that there is again a great jump in passing to $CsCaF_3$. In other words, the presence of a nonzero A_{ML} produces large changes in the values of f_p but not in the $f_p(R)$ function because A_{ML} is near independent of R.

Given the uncertainty in the final values of f_p indicated in Table V, we cannot detect a definite trend in the variation of this parameter with R. Our results give $f_p = 0.60 \pm 0.20$ % in the range $2.07 \leq R \leq 2.16$ Å.

Let us now compare these empirical results with the SCF calculations of the preceding section. As we have

TABLE V. f_p covalency parameter (in percent) computed by means of different approximations. A_p, A_d, and A_{ML} are in units of 10^{-4} cm^{-1}. A_d has been computed through Eq. (10) with $N_t = N_e = 1$.

System	A_p	R_0	$A_{ML}=0$; no ligand relaxation A_d	f_p
Mn^{2+}:$KZnF_3$	3.05±0.02[a]	2.026	2.95	0.12±0.02
Mn^{2+}:$RbCdF_3$	2.80±0.03[b]	2.200	2.30	0.58±0.03
Mn^{2+}:$CsCaF_3$	2.91±0.03[c]	2.262	2.12	0.92±0.03
			$A_{ML}=0$; ligand relaxation	
		R	A_d	f_p
		2.07±0.01[d]	2.78±0.10	0.31±0.14
		2.12±0.01[d]	2.56±0.10	0.28±0.15
		2.16±0.01[e]	2.45±0.10	0.54±0.15
			$A_{ML}\neq 0$; ligand relaxation	
	R	A_d	A_{ML}	f_p
	2.07±0.01	2.78±0.10	0.21±0.05	0.56±0.20
	2.12±0.01	2.56±0.10	0.18±0.05	0.49±0.21
	2.16±0.01	2.45±0.10	0.17±0.05	0.73±0.21

[a]Reference 12.
[b]130 K, cubic phase, Ref. 14.
[c]Reference 13.
[d]References 31–33.
[e]Reference 30.

seen, the effects of the lattice potential on f_p in these calculations are so small that we can discuss the cluster-*in-vacuo* results without loss of detail. In the range of R examined in Table V the SCF values of f_p show a decrease of about 16%.

On the other hand, an interesting aspect of the SCF calculation is that we can explore a wider range of metal-ligand distances. When we look at the range $1.90 \leq R \leq 2.33$ Å, much larger than experimentally observed, we appreciate the continuous decrease of f_p with increasing R shown in Fig. 1. This variation is much smaller than that obtained for f_s. For instance, in passing from 1.90 to 2.33 Å, f_p reduces from 3.60% to 1.89% but f_s changes from 1.4% to 0.3% (see Fig. 1).

A final comparison between the SCF results and the values in Table V involves the f_p values themselves. The SCF result of $f_p = 2.67 \pm 0.18$ % obtained in the range of R considered in Table V is about 5 times larger than the empirical one, 0.60 ± 0.20 %. This overestimation may be due, in part, to an underestimation of f_π. Such underestimation was reported for CrF_3 by Barandiarán and Pueyo:[57] they obtained $f_\pi(\text{SCF}) = 1.73\%$ versus $f_\pi(\text{expt}) = 2.6\%$.

We can conclude that the empirical value of f_p in these perovskites is 0.60 ± 0.20 % and that both SCF calculations and empirical analysis support the idea of small variations of this parameter with R in the range $2.07 \leq R \leq 2.16$ Å, although SCF calculations over a larger range of R show a clear decrease of f_p with increasing R. Ligand relaxation is a determining factor in reaching this conclusion. The A_{ML} term has smaller effects on the $f_p(R)$ function but it is very important in setting the value of f_p.

V. CONCLUDING REMARKS

A particular emphasis has been put in this work on the obtaining of empirical values of f_p from magnetic-resonance spectroscopy. The effect of the ligand relaxation accompanying the metallic substitution has been quantitatively evaluated. The usually neglected metal-ligand contribution to the shf tensor has also been taken in account. These two factors may produce very large changes in the values of f_p obtained through the traditional analysis. The ligand relaxation may alter not only the values of f_p but also the function $f_p(R)$.

In the analysis of ENDOR data for the $KZnF_3$, $RbCdF_3$, and $CsCaF_3$ perovskites doped with Mn^{2+} we have found that f_p does not show any definite trend when R changes from 2.07 to 2.16 Å. On the other hand, HFR results obtained in this work for a larger range of distances show that f_p decreases as $R^{-3.2}$. This HFR result may be useful if measurements of the shf tensor at very high pressures become available.

The question of the separate values of f_σ and f_π for the $(MnF_6)^{4-}$ cluster is, however, not fully resolved. The theoretical values of f_σ near the equilibrium geometry, collected in Table I, range from 0.7% to 3.0%. The only value for the sum $f_\sigma + 2f_\pi + f_s$ obtained in neutron-diffraction experiments[5] is 3.3%. Combining this sum with our value for $f_p = 0.60\%$, and taking $f_s = 0.5\%$,[13] we find $f_\sigma = 1.33\%$ and $f_\pi = 0.73\%$. These numbers agree with those calculated by Adachi *et al.*[25] ($f_\sigma = 1.4\%$, $f_\pi = 0.6\%$). In order to be sure of these figures that provide us with an f_σ value comparable to that determined in Ni^+:LiF,[53] it is clear that additional neutron-diffraction experiments would be desirable.

Simultaneous consideration of the neutron-diffraction data by Nathans *et al.*[5] and the present results for f_p does not support the conclusion by Ziaei and Owen, derived from the analysis of the supertransferred spin density on Cd in Mn^{2+}:$CsCdF_3$,[11] of $f_\sigma = 4.3\%$ and $f_\pi = 3.8\%$ for $(MnF_6)^{4-}$. This value of f_σ is hard to accept when compared to the value $f_\sigma = 4.2\%$ for the distorted $(CuF_6)^{4-}$ involving a cation with an optical electronegativity much larger than that of Mn^{2+}. Also, we recall that Aoki *et al.*[13] suggested that these high values of f_σ and f_π are difficult to reconcile with the small value of the trace of the shf tensor related to the next-nearest-neighbor fluoride ions in $CsCaF_3$.

Ligand relaxation plays a key role in the determination of the empirical covalency parameters in doped perovskites. However, in concentrated materials like $RbMnF_3$ this effect disappears. The tradiational analysis of this compound, with $A_{\text{ML}} = 0$, gives $f_p = 0.33 \pm 0.18$ %.[6] When the metal-ligand term is taken into account ($A_{\text{ML}} = 0.2 \times 10^{-4}$ cm^{-1}) we obtain $f_p = 0.60 \pm 0.23$ %, a value quite consistent with that reported in this work for other perovskites *doped* with Mn^{2+}. This result suggests that the sharing of ligand ions by neighbor clusters in $RbMnF_3$ does not produce significant differences in covalency with respect to what is observed in isolated clusters dissolved in a host lattice. This result was also observed in the analysis of f_s (Ref. 30) and optical spectra[32,33] of this type of Mn^{2+}-doped fluoroperovskites. The effect may likely be related to the high ionicity of the Mn^{2+}—F^- bond and should be viewed more as an exception than as a rule.

Finally, we would like to refer to the ENDOR measurements by Yosida on $LiBaF_3$.[15] This material shows the inverse perovskite structure with a lattice parameter $a = 3.995$ Å. In this case the Mn^{2+} ion substitutes a Li^+ ion. Yosida reported $A_s = 18.47 \pm 0.03 \times 10^{-4}$ cm^{-1} and $A_p = 3.67 \pm 0.03 \times 10^{-4}$ cm^{-1}. From this A_s value and following the procedure of Ref. 30 we determine the Mn^{2+}-F^- distance to be $R = 2.06$ Å. Thus, we find in this system an outwards ligand relaxation analogous to that in $KZnF_3$ (Table V). Nevertheless, from the observed value of A_p and $R = 2.06$ Å, we derive $f_p = 1.3\%$, i.e., twice the value reported in this work for normal perovskites. It is interesting to conjecture that this difference is simply due to the different structure of the host lattice. In any case, it appears that further experimental and theoretical study of this type of crystals is necessary for reaching definite conclusions on the covalency in inverse perovskites. In line with this, we are planning to extend the present study to the Mn^{2+} ion in different types of crystals and to the isoelectronic Cr^+ and Fe^{3+} ions as well.

ACKNOWLEDGMENTS

The authors want to express their thanks to Dr. Fernando Rodríguez and Dr. Evelio Francisco for their help in several calculations. Financial support from Comisión Asesora de Investigación Científica y Técnica under Project Nos. 3056/83 and 2880/83 is gratefully acknowledged.

[1]R. G. Shulman and S. Sugano, Phys. Rev. **130**, 506 (1963).
[2]S. Ogawa, J. Phys. Soc. Jpn. **15**, 1475 (1960).
[3]R. G. Shulman and K. Knox, Phys. Rev. **119**, 94 (1960).
[4]T. P. P. Hall, W. Hayes, R. W. H. Stevenson, and J. Wilkens, J. Chem. Phys. **38**, 1977 (1963).
[5]R. Nathans, G. Will, and D. E. Cox, in *Proceedings of the International Conference on Magnetism, Nottingham, 1965* (Institute of Physics and Physical Society, London, 1964), p. 327.
[6]M. B. Walker and R. W. H. Stevenson, Proc. R. Soc. London **87**, 35 (1966).
[7]J. Owen and J. H. M. Thornley, Rep. Prog. Phys. **29**, 675 (1966), and references quoted therein.
[8]P. A. Narayana, Phys. Rev. B **10**, 2676 (1974).
[9]B. C. Tofield, J. Phys. (Paris) Colloq. **C6**-539 (1976), and references quoted therein.
[10]J. J. Rousseau, A. Leblé, and J. C. Fayet, J. Phys. (Paris) **39**, 1215 (1978).
[11]M. E. Ziaei and J. Owen, J. Phys. C **9**, L529 (1976).
[12]R. K. Jeck and J. J. Krebs, Phys. Rev. B **5**, 1677 (1972).
[13]H. Aoki, M. Arakawa, and T. Yosida, J. Phys. Soc. Jpn. **52**, 2216 (1983).
[14]P. Studzinski and J. M. Spaeth, Radiat. Eff. **73**, 215 (1983).
[15]T. Yosida, J. Phys. Soc. Jpn. **49**, 127 (1980).
[16]A. J. Freeman and D. E. Ellis, Phys. Rev. Lett. **24**, 516 (1970).
[17]E. Simanek and K. A. Müller, J. Phys. Chem. Solids **31**, 1027 (1970).
[18]R. D. Brown and P. G. Burton, Theor. Chim. Acta **18**, 309 (1970).
[19]T. F. Soules and J. W. Richardson, Phys. Rev. Lett. **25**, 110 (1970).
[20]O. Matsuoka, J. Phys. Soc. Jpn. **28**, 1296 (1970).
[21]O. Matsuoka and T. L. Kunii, J. Phys. Soc. Jpn. **30**, 1771 (1971).
[22]S. Larsson, Phys. Lett. **45A**, 185 (1973).
[23]S. Larsson and J. W. D. Connolly, J. Chem. Phys. **60**, 1514 (1974).
[24]D. W. Clack and M. Monshi, Rev. Roum. Chim. **23**, 495 (1976).
[25]H. Adachi, S. Shiokawa, M. Tsukada, C. Satoko, and S. Sugano, J. Phys. Soc. Jpn. **47**, 1528 (1979).
[26]K. N. Shrivastava, Physica (Utrecht) **100B**, 67 (1980).
[27]J. Emery, A. Leblé, and J. C. Fayet, J. Phys. Chem. Solids **42**, 789 (1981).
[28]J. Emery and J. C. Fayet, Solid State Commun. **42**, 683 (1982).
[29]J. W. Richardson, T. F. Soules, D. M. Vaught, and R. R. Powell, Phys. Rev. B **4**, 1721 (1971).
[30]M. T. Barriuso and M. Moreno, Phys. Rev. B **29**, 3623 (1984).
[31]A. Leblé, these d'Etat, Université du Maine, 1982.
[32]F. Rodríguez and M. Moreno, J. Chem. Phys. **84**, 692 (1986).
[33]F. Rodríguez, M. Moreno, A. Tressaud, and J. P. Chaminade, Cryst. Lattice Defects Amorph. Mater. **16**, 221 (1987).
[34]M. Flórez, G. Fernández Rodrigo, E. Francisco, V. Luaña, J. M. Recio, J. F. Van der Maelen, L. Pueyo, M. Bermejo, M. Moreno, J. A. Aramburu, and M. T. Barriuso, Cryst. Lattice Defects Amorph. Mater. **15**, 53 (1987).
[35]J. W. Richardson, W. C. Nieuwpoort, R. R. Powell, and W. F. Edgell, J. Chem. Phys. **36**, 1057 (1962).
[36]J. W. Richardson, R. R. Powell, and W. C. Nieuwpoort, J. Chem. Phys. **38**, 796 (1963).
[37]M. Flórez, L. Seijo, and L. Pueyo, Phys. Rev. B **34**, 1200 (1986).
[38]L. Seijo, Doctoral thesis, Universidad de Oviedo, 1983.
[39]B. L. Kalman and J. W. Richardson, J. Chem. Phys. **55**, 4443 (1971).
[40]Y. Sakai and S. Huzinaga, J. Chem. Phys. **76**, 2552 (1982), and references quoted therein.
[41]L. Seijo, Z. Barandiarán, V. Luaña, and L. Pueyo, J. Solid State Chem. **61**, 269 (1986).
[42]V. Luaña, G. Fernández Rodrigo, E. Francisco, L. Pueyo, and M. Bermejo, J. Solid State Chem. **66**, 263 (1987).
[43]V. Luaña, E. Francisco, M. Flórez, J. M. Recio, and L. Pueyo, J. Chim. Phys. (Paris) **84**, 863 (1987).
[44]M. Flórez, M. Bermejo, V. Luaña, E. Francisco, J. M. Recio, and L. Pueyo, J. Chim. Phys. (Paris) **84**, 855 (1987).
[45]V. Luaña, and L. Pueyo, J. Mol. Struct. (Theochem.) (to be published).
[46]V. Luaña, G. Fernández Rodrigo, M. Flórez, E. Francisco, J. M. Recio, J. F. Van der Maelen, L. Pueyo, and M. Bermejo, Cryst. Lattice Defects Amorph. Mater. **15**, 19 (1987).
[47]V. Luaña (private communication).
[48]C. K. Jorgensen, *Modern Aspects of Ligand Field Theory* (North-Holland, Amsterdam, 1971), Chap. 23.
[49]E. Francisco (private communication).
[50]J. S. Griffith, *The Theory of Transition-Metal Ions* (Cambridge University Press, Cambridge, 1971).
[51]J. A. Aramburu and M. Moreno, J. Chem. Phys. **83**, 6071 (1985).
[52]J. Weber and R. Lacroix, Helv. Phys. Acta **44**, 181 (1971).
[53]M. Moreno, J. A. Aramburu, and M. T. Barriuso, J. Phys. C **19**, L315 (1986).
[54]E. Clementi and C. Roetti, At. Data Nucl. Data Tables **14**, 177 (1974).
[55]F. J. Adrian, A. N. Jette, and J. M. Spaeth, Phys. Rev. B **31**, 3923 (1985).
[56]C. K. Jorgensen, Prog. Inorg. Chem. **12**, 101 (1970).
[57]Z. Barandiarán and L. Pueyo, J. Chem. Phys. **80**, 1597 (1984).